10/1-16-96 JS①

SANDIA REPORT

SAND96-8449 • UC–401
Unlimited Release
Printed December 1995

The Chemistry of Boron and Titanium Diboride Formation: Decomposition of $TiCl_4$ and BCl_3 in Hydrogen and Helium

(To be published in *Covalent Ceramics III - Science and Technology of Non-Oxides*, the Materials Research Society, Vol. 410, 1996.)

T. H. Osterheld, M. D. Allendorf

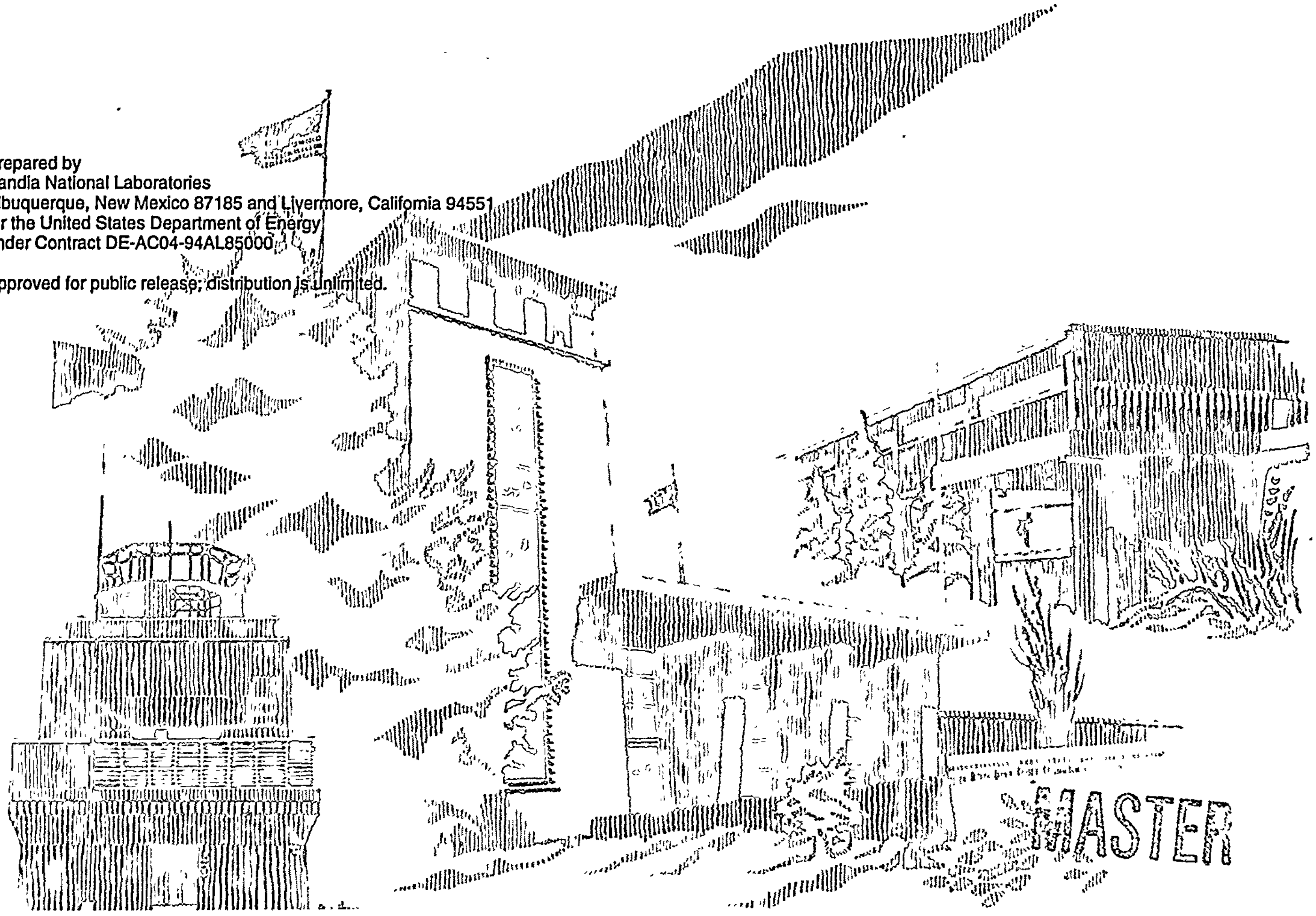

Prepared by
Sandia National Laboratories
Albuquerque, New Mexico 87185 and Livermore, California 94551
for the United States Department of Energy
under Contract DE-AC04-94AL85000

Approved for public release; distribution is unlimited.

MASTER

SF2900Q(8-81)

DISTRIBUTION OF THIS DOCUMENT IS UNLIMITED 35

This report has been reproduced from the best available copy.

Available to DOE and DOE contractors from:

Office of Scientific and Technical Information
P. O. Box 62
Oak Ridge, TN 37831

Prices available from (615) 576-8401, FTS 626-8401

Available to the public from:

National Technical Information Service
U.S. Department of Commerce
5285 Port Royal Rd.
Springfield, VA 22161

UC-401

SAND96-8449
Unlimited Release
Printed December 1995

THE CHEMISTRY OF BORON AND TITANIUM DIBORIDE FORMATION: DECOMPOSITION OF $TiCl_4$ AND BCl_3 IN HYDROGEN AND HELIUM*

THOMAS H. OSTERHELD AND MARK D. ALLENDORF
Sandia National Laboratories, Mail Stop 9052
Livermore, CA 94551-0969

ABSTRACT

Measurements of the decomposition of mixtures of boron trichloride (BCl_3), titanium tetrachloride ($TiCl_4$), and hydrogen at elevated temperatures are presented. The decomposition of BCl_3 with hydrogen appears to drive the chemistry in this system. The species depositing boron on the surface contains at least 2 chlorine atoms. Once deposited, the surface chlorine is removed by reaction with hydrogen to form HCl and, presumably, surface B-H bonds.

---

* This work was supported by the DoD Advanced Research Projects Agency.

INTRODUCTION

The chemical vapor deposition (CVD) of boron by the decomposition of boron trichloride (BCl_3) in hydrogen (H_2) (Reaction 1) is of intense interest for the manufacture of boron fibers, which are used to reinforce polymeric and metallic composites [1]. The reaction of BCl_3 with $TiCl_4$ and H_2 to generate TiB_2 (Reaction 2) is also of interest for the manufacture of coatings to protect ceramic fibers from chemical attack during composite processing:

$$BCl_3 + \frac{3}{2}H_2 = B(c) + 3HCl \tag{1}$$

$$2BCl_3 + TiCl_4 + 5H_2 = TiB_2 + 10HCl \tag{2}$$

In general, what is known or proposed about the chemistry in these systems has arisen from equilibrium calculations and modeling of the deposition process [2-7]. Two of these reports suggest that BCl_2H may form in the gas phase but not $BClH_2$ [2, 5], and that BCl_2H may play a role in the deposition process.

In this work, we used a high-temperature flow reactor (HTFR) equipped with a mass spectrometer to monitor the concentrations of gas-phase species during the reaction of BCl_3 and/or $TiCl_4$ as a function of temperature, residence time, and mixture composition. The data obtained suggest that a surface reaction involving BCl_3 and H_2 is responsible for BCl_3 removal from the gas phase and for accelerated rates of $TiCl_4$ reaction in the presence of these two gases. The experiments also demonstrate that $BHCl_2$ forms, confirming the earlier prediction. The results are used to identify several reactions that occur during the deposition process.

EXPERIMENTAL METHODS

A schematic of the HTFR is shown in Figure 1. Reactions occur within a 100-cm long graphite tube (5.0 cm ID) enclosed within a water-cooled, insulated vacuum chamber. Three independently controlled graphite heating elements surround the tube and heat the gases flowing within it to temperatures up to 1500 K. Reactor pressure is measured and controlled (to ± 0.1 torr) by a pressure transducer coupled to a throttle valve in the vacuum line. BCl_3 and $TiCl_4$ enter the HTFR through a water-cooled injector and mix with the preheated carrier gas. The injector is movable, allowing the reactant residence time to be varied with respect to a quartz probe used for sampling. Delivery of gases to the reactor is controlled by calibrated mass flow controllers. Initial concentrations of 2-7% for BCl_3 and $TiCl_4$ were used. For $TiCl_4$, the vapor pressure above a temperature-controlled liquid reservoir was used to drive a mass flow controller.

Gases are extracted from the HTFR by a quartz sampling probe inserted into the center of the flow in the diagnostic region. The pressure inside the probe was maintained at 2.0 ± 0.1 torr by a pressure transducer/throttle valve combination. Once extracted by the probe, the gases flow past a 200-μm orifice attached to an Extrel EXM-500 quadrupole mass spectrometer system where a small portion is expanded into the mass spectrometer for analysis using 70 eV ionization energy. The accuracy of the mass and peak height calibration was verified by measuring the mass spectra of perfluorotributylamine and boron trichloride.

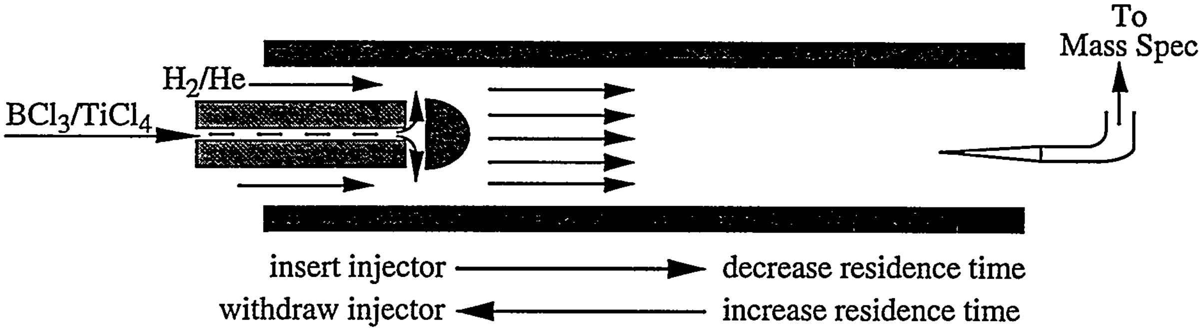

Figure 1: Schematic of high-temperature flow reactor experiment.

In a typical experiment, a carrier gas consisting of helium or hydrogen (or a mixture of the two) entered the reaction tube and was preheated to the reactor temperature by the first heating element. BCl_3 and/or $TiCl_4$ were then mixed with the hot carrier gas, following transport to the reactor through the injector. Under the experimental conditions adopted here, both mixing and thermal equilibration of the injected species with the preheated carrier gas are rapid compared with the time allowed for reaction to occur. Gas residence times were determined from the average convective velocity, assuming plug-flow conditions [8].

Concentrations were measured for each species relative to the m/z 40 signal from an internal standard of argon. The calibration factors for BCl_3 and $TiCl_4$ relative to argon were determined from known concentrations of these gases under non-reacting conditions. The calibration factor for HCl relative to argon was calculated from the relative ionization cross-sections, after correcting for the isotopic distribution of each species and fragmentation of HCl in the mass spectrometer. Since pure BCl_2H is not available and its ionization cross section is unknown, the calibration factor for this molecule was estimated by assuming that one mole of BCl_2H is generated for each mole of BCl_3 observed to react in HTFR experiments at low temperatures (300-500 °C; a reasonable assumption--see Reaction 3 and the Discussion section). The calibration factor is the average of several measurements in this temperature range, all of which gave similar numbers. BCl_3 and $TiCl_4$ were monitored by their molecular-ion signals at m/z 116 and 190 respectively; HCl was monitored by its molecular ion signal at either m/z 36 or 38, and BCl_2H was monitored by its fragment ion at m/z 47 ($BClH^+$).

RESULTS AND DISCUSSION

Experiments in helium demonstrate that the unimolecular decomposition of BCl_3 and $TiCl_4$ is negligible. At temperatures up to 1363 K and a total pressure of 40 torr, no decomposition of either species is observed for residence times between 0 and 330 ms. This result is not surprising for BCl_3, given its large bond dissociation energy (BDE) (118 kcal mol^{-1} [9]). However, it suggests that Ti-Cl BDE of 82.4 kcal mol^{-1} for $TiCl_4$ calculated from heats of formation given in the *JANAF Tables* [10] is too low [11].

In contrast, both BCl_3 and $TiCl_4$ react in the presence of hydrogen, with BCl_3 reacting more rapidly than $TiCl_4$. Concurrent formation of HCl is also detected, with the amount formed increasing with residence time. Rates for these reactions were extracted from concentration data obtained at two different gas residence times (i.e., two different injector positions) by assuming simple first-order kinetics (the actual kinetics are likely more complex) and are given in Table I. These results indicate that BCl_3 is responsible for the initiation of chemical reactions in this system, since it reacts readily on its own in hydrogen and is required for significant $TiCl_4$ decomposition to occur. Most of the remainder of this paper will therefore concentrate on the reactions of BCl_3.

Table I: Dependence of decomposition rate on initial mixture composition (20 torr).

Reaction	k_{BCl3} (s^{-1})	k_{TiCl4} (s^{-1})	Temp. (K)
$BCl_3 + TiCl_4 + He \rightarrow$ products	$< 0.16\ s^{-1}$	$< 0.16\ s^{-1}$	1363
$BCl_3 + H_2 \rightarrow$ products	$\sim 1.5 - 3\ s^{-1}$		1263
$TiCl_4 + H_2 \rightarrow$ products		$\sim 0.06\ s^{-1}$	1263
$BCl_3 + TiCl_4 + H_2 \rightarrow$ products	$\sim 2 - 3\ s^{-1}$	$\sim 0.4 - 0.8\ s^{-1}$	1263

In addition to detecting HCl as a reaction product, small amounts of BCl_2H are also found when BCl_3 reacts with hydrogen (Figure 2) (the non-zero HCl signal at time zero is due to reaction of BCl_3 with adsorbed water in the gas-transfer lines). This provides experimental confirmation of earlier reports [2, 5] that this molecule forms when BCl_3 reacts with hydrogen. No other boron-containing species were detected, including $BClH_2$. Identification of the BCl_2H product was not straightforward, since the major molecular-ion peaks at m/z 82 and 84 are obscured by isotopes of the much larger BCl_2^+ signal produced by BCl_3. Although the ratio of the m/z 82 signal (which includes contributions from $^{11}B^{35}Cl_2H^+$ and $^{10}B^{35}Cl^{37}Cl^+$) to the m/z 116 signal ($^{11}B^{35}Cl_3^+$) increases as a function of residence time, suggesting that a product is being formed, the changes are small and difficult to quantify. However, the signal at m/z 47, which corresponds to the $BClH^+$ fragment of BCl_2H, has only a minor contribution from BCl_3 fragmentation and can thus be used to quantify the amount of BCl_2H formed. Contributions to m/z 47 are also possible from $BClH_2$; however, the parent-signal of $BClH_2$ at m/z 50 does not exhibit the same residence-time behavior as the signal at m/z 47. We thus conclude that no $BClH_2$ is formed.

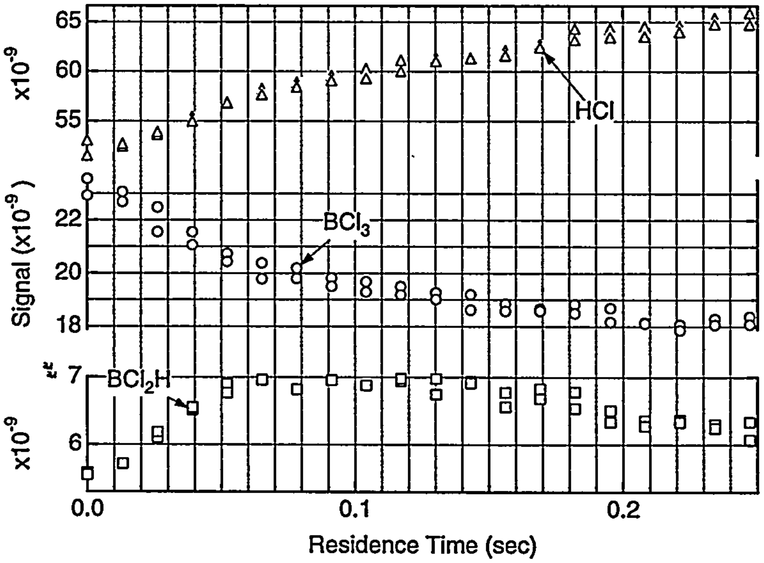

Figure 2: Dependence of BCl_3, BCl_2H, and HCl signals on residence time at 973 K and 22 torr for 7% BCl_3 and 67% H_2.

Thus, the net reaction between BCl_3 and H_2 can be described by Reaction (3):

$$BCl_3 + H_2 \leftrightarrow BCl_2H + HCl \qquad \Delta H^\circ(298\ K) = 15.8\ kcal\ mol^{-1} \qquad (3)$$

Although Reaction 3 involves only gas-phase species, *ab initio* calculations (discussed in detail elsewhere [11]) performed to determine upper limits for this reaction rate indicate that the gas-phase reaction is too slow to account for the observed rate of BCl_3 loss. Radical-based chemistry involving hydrogen atoms can also be eliminated because the temperatures are too low to produce significant H-atom concentrations. Thus, we conclude that Reaction 3 must be a surface-catalyzed process.

Experiments in which the BCl_3 signal is monitored as a function of residence time suggest that Reaction 3 approaches an equilibrium. This is shown in Figure 3, where it can be seen that the BCl_3 concentration initially decreases as a function of residence time, then levels off at a distinctly non-zero value at residence times greater than 300 msec. The three curves in Figure 3 also show that the final concentration of BCl_3 depends on the H_2 concentration, with higher concentrations of H_2 causing more BCl_3 to react. The observed BCl_3 concentrations are in reasonable agreement with the concentrations predicted by equilibrium. Table II compares the extent of decomposition observed experimentally for 3.3% BCl_3/33% H_2 (in helium) to that calculated from the equilibrium constant determined by ΔG° [9] for Reaction 3 .

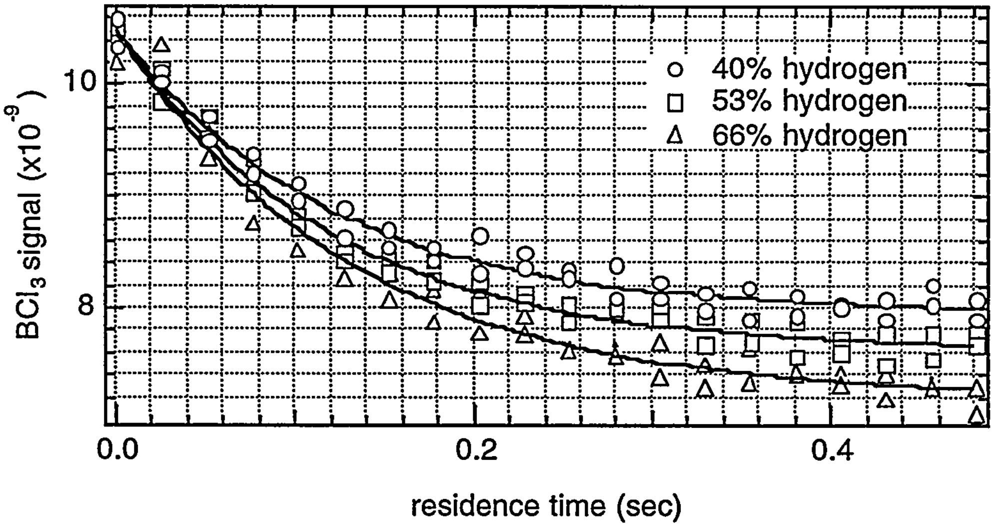

Figure 3: Dependence of BCl_3 signal on residence time at 963 K and 42 torr for 3% BCl_3 in a mixture of helium and hydrogen. The three different data sets denote different hydrogen concentrations.

Table II: Comparison observed percent BCl_3 reacted with equilibrium prediction.

Temperature (K)	ΔG° (kcal mol^{-1})	ΔBCl_3 (equilibrium)[a]	ΔBCl_3 (observed)
673	11.5	4.4 %	5-6 %
773	11.0	8.7 %	8-9 %

[a] Calculation accounts for the non-zero input concentration of HCl.

The dependence of the BCl_2H signal on residence time shown in Figure 2 indicates that this species must undergo additional reactions, since its concentration reaches a maximum between 50 and 150 msec. No new boron-containing gas-phase species are detected, however, as the BCl_2H disappears. Thus, a surface reaction is likely responsible for BCl_2H removal from the gas phase. To support this conclusion, we now describe experiments in which the concentrations of BCl_3 and HCl were simultaneously monitored as a function of injector position. The results show (Figure 4) that two molecules of HCl are evolved for every molecule of BCl_2H consumed.

In these experiments, BCl_3 was injected at 690 °C into preheated carrier gas composed of 67% hydrogen/33% helium. At the beginning of an experiment, the injector was fully withdrawn from the reactor (see Figure 1), maximizing both the residence time of BCl_3 (τ) and the surface area to which it is exposed. This corresponds to the clock time $t = 0$ minutes and residence time $\tau = 0.48$ seconds in Figure 4. At this point, BCl_3 reacts with hydrogen via Reaction 3 to generate HCl and BCl2H (not shown for clarity). Later in the experiment ($t \approx 5.7$ min), the injector was fully inserted into the reactor, reducing τ to essentially to zero (hydrogen, however, was still flowing through the entire length of the reactor). As a result, the concentration of BCl_3 increased while the concentration of HCl decreased. The magnitude of the concentration change for both species is approximately the same ($\Delta BCl_3 \approx 8000$ ppm and $\Delta HCl \approx 9000$ ppm), indicating that, initially, one mole of HCl is generated for each mole of BCl_3 that decomposes. Thus, these observations are consistent with the stoichiometry of Reaction 3.

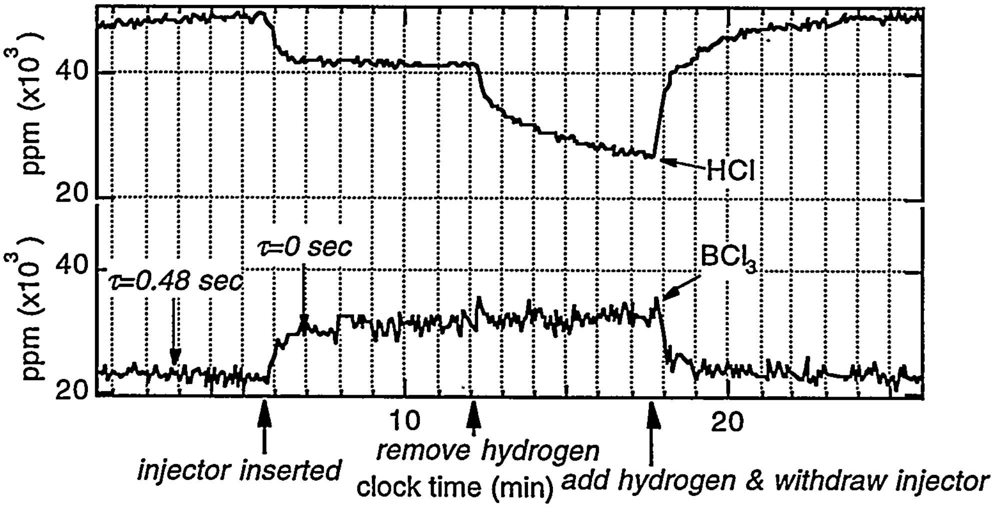

Figure 4: Dependence of the BCl_3 and HCl signals as several reaction parameters are changed at 963 K and 42 torr with 3% BCl_3/67% H_2/30% He. The x-axis indicates elapsed time of the experiment and has no relation to the residence time of BCl_3 in the reactor.

At a still later time in the experiment ($t \approx 12$ min) the hydrogen in the carrier gas was replaced by helium. This has little effect on the BCl_3 concentration, since BCl_3 is no longer consumed by Reaction 3 because of the reduction in τ that occurred at $t \approx 5.7$ min. However, a dramatic drop in the HCl signal is observed. This indicates that hydrogen, which continued to flow through the entire length of the reactor, reacts with adsorbed chlorine-containing species on the walls, forming HCl. Quantitatively, the removal of hydrogen from the carrier gas results in a change in the HCl concentration ($\Delta HCl \approx 15{,}000$ ppm) that is approximately twice the amount of BCl_3 that reacts ($\Delta BCl_3 = 8000$ ppm) to produce BCl_2H. Thus, the reaction of BCl_2H with the reactor walls results in the formation of one or more adsorbed species containing a total of two chlorine atoms, consistent with the amount of HCl evolved by reaction with H_2.

When $TiCl_4$ is added to the system HCl generation occurs even more rapidly, with the full theoretical yield of HCl molecules (three from BCl_3 and four from $TiCl_4$) detected for each molecule of $TiCl_4$ or BCl_3 that reacts. This was determined by an experiment similar to that described in Figure 4. Figure 4 shows, however, that when $TiCl_4$ is not present, only one equivalent of HCl is formed by changing the residence time of BCl_3. Thus, $TiCl_4$ must react with adsorbed boron species to yield products that react more readily with hydrogen to generate HCl.

CONCLUSIONS

Several conclusions relevant to CVD processes that use BCl_3 can be drawn from these experiments. First, reactions can occur between BCl_3 and H_2 on the surface that produce a new gas-phase species, BCl_2H. Although this is hardly a new concept in surface science, it does run counter to the often-made assumption in CVD modeling that reactions of gas-phase species with the deposition surface are irreversible and result in the deposition of one or more atoms. In the case examined here, the product molecule that desorbs is later readsorbed by the reactor walls, presumably depositing boron on the surface. Thus, even though gas-phase reactions may be slow, surface processes can create new species that alter the composition of the gas-phase and, consequently, change the relative concentrations of species forming the deposit. A second, related conclusion is that BCl_3 must be adsorbed by the surface for BCl_2H to form. No evidence of this was found in the experiments in helium carrier gas; evidently, the amount adsorbed is too small for a concentration change to be observed. The amount is sufficient, however, for BCl_2H to be immediately produced when H_2 is introduced into the carrier gas. A third conclusion is that BCl_3 adsorption appears to chemically activate the surface, since $TiCl_4$ reacts faster in the presence of both BCl_3 and H_2.

The reactions that appear to occur between BCl_3 and H_2 can be summarized as follows:

$$BCl_3 + \text{surface} \leftrightarrow Cl_3B\text{-(surf)} \tag{4}$$

$$H_2 + Cl_3B\text{-(surf)} \leftrightarrow Cl_2HB\text{-(surf)} + HCl \tag{5}$$

$$BCl_2H + \text{surface} \leftrightarrow Cl_2HB\text{-(surf)} \tag{6}$$

$$Cl_2(X)B\text{-(surf)} + H_2 \leftrightarrow H\text{-}BCl(X)\text{-(surf)} + HCl \tag{7}$$

In these equations, X represents H, Cl, or another boron atom on the surface and "surf" indicates an atom (presumably boron) on the surface. Reaction 5 may occur as written; however, it is also possible that H_2 must be adsorbed prior to reaction with an adsorbed BCl_3 molecule. It is conceivable that Reactions 6 and 7 involve a 1,2-elimination with a transition state such as the one shown in Reaction 8 (Y represents H, Cl, or a surface boron atom):

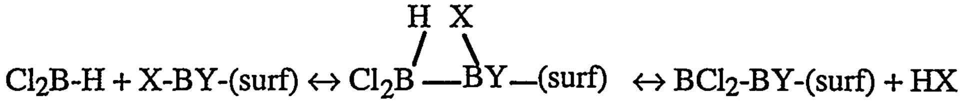

$$Cl_2B\text{-}H + X\text{-}BY\text{-}(surf) \leftrightarrow Cl_2\overset{H}{B}—\overset{X}{B}Y—(surf) \leftrightarrow BCl_2\text{-}BY\text{-}(surf) + HX \qquad (8)$$

The heat of reaction for these processes is not known. However, *ab initio* calculations indicate that the analogous gas-phase reactions, in which either H_2 or HCl are eliminated, are endothermic by modest amounts; ~4 kcal mol^{-1} and ~20 kcal mol^{-1}, respectively [11]. If the thermodynamics of the surface reaction are similar, typical CVD temperatures should provide sufficient energy for Reaction 8 to proceed at rates that are fast on the time scale of many deposition processes.

The nature of the reactions subsequent to Reaction 8 that remove chlorine from the surface and incorporate boron into the lattice are not clear from the experiments conducted here. We are currently performing additional *ab initio* calculations to evaluate the feasibility of potential deposition mechanisms, based on analogous gas-phase reactions. Additional experiments will also be required to fully characterize the relevant deposition chemistry.

REFERENCES

1. M. Schwartz, Composite Materials Handbook. (McGraw-Hill, Inc., New York, 1992).
2. T. M. Besmann, K. E. Spear, *Journal of the Electrochemical Society* **124**, 790 (1977).
3. H. Rebenne, R. Pollard, *Journal of the Electrochemical Society* **132**, 1932 (1985).
4. L. Vandenbulcke, G. Vuillard, *Journal of the Electrochemical Society* **124**, 1931 (1977).
5. H. E. Carlton, J. H. Oxley, E. H. Hall, J. M. Blocher Jr., J. C. Withers, Ed., *Proc. of the 2nd Int. Conf. on Chemical Vapor Deposition* (The Electrochemical Society, 1970), pp. 209.
6. J.-O. Carlsson, T. O. Sedgwick, H. Lydtins, Ed., *Proc. of the 7th Int. Conf. on Chemical Vapor Deposition* (The Electrochemical Society, 1979), vol. 79, pp. 332.
7. M. Nadal, T. Grenet, F. Teyssandier, *J. De Phys. IV C3* **3**, 511 (1993).
8. L. F. Keyser, *Journal of Physical Chemistry* **88**, 4750 (1984).
9. H. B. Schlegel, S. J. Harris, *Journal of Physical Chemistry* **98**, 11178 (1994).
10. M. W. J. Chase, et al., *Journal of Physical and Chemical Reference Data* **14**, 860 (1985).
11. T. H. Osterheld, M. D. Allendorf, C. F. Melius, to be published.

INITIAL DISTRIBUTION
UNLIMITED RELEASE

Dr. Peter Angelini
Bldg. 4515
Oak Ridge National Laboratories
P.O. Box 2008, 1 Bethel Valley Road
Oak Ridge, TN 37831-6065

Dr. Sara Dillich
Adv. Industrial Concepts Div., EE-232
U.S. DOE - EE
Forrestal Building
1000 Independence Avenue
Washington, DC 20585

Dr. Charles A. Sorrell
Adv. Industrial Concepts Div., EE-232
U.S. DOE - EE
Forrestal Building
1000 Independence Avenue
Washington, DC 20585

Dr. Theodore M. Besmann
Oak Ridge National Laboratories
P.O. Box 2008
Oak Ridge, TN 37831-6063

Dr. F. D. Gac
Los Alamos National Laboratory
G771
P.O. Box 1663
Los Alamos, NM 87545

Dr. Greg Glaitzmaier
NREL
1617 Cole Blvd.
Golden, CO 80401

Dr. Suleyman A. Gokoglu
NASA Lewis Research Center
Mail Stop 106-1
Clevland, OH 44135

Dr. John W. Hastie
National Inst. of Standards &
Technology
Metallurgy Division
B106/223
Gaithersburg, MD 20899

Dr. Gerd M. Rosenblatt
Building 50A, Room 4119
Lawrence Berkeley Laboratory
1 Cyclotron Road
Berkeley, CA 94720

Dr. Michael Zachrich
National Institute of Standards and
Technology
Building 221,Rm. B312
Gaithersburg, MD 20899

Prof. Peter B. Armentrout
Department of Chemistry
University of Utah
Henry Eyring Building
Salt Lake City, UT 84112

Professor Richard Axelbaum
Dept. of Mechanical Engineering
Washington University
St. Louis, MO 63130

Prof. Dieter Baeuerle
Johannes-Kepller-Universitat Linz
Institu fur Angewandte Physik
A-4040 Linz
Austria

Prof. C. Bernard
Laboratoire de Thermodynamique
ENSEEG
BP.75,38402
St. Martin d'Heres
France

Professor John I. Brauman
Department of Chemistry
Stanford University
Stanford, CA 94305

Dr. Ken Brezinsky
Department of Mechanical & Aerospace
Engineering
Princton University
Engineering Quadrangle, D329
Princeton, NJ 08544

Professor Mark A. Capelli
Department of Mechanical Engineering
Stanford University
Building 500
Stanford, CA 94305-1901

Prof. Jan-Otto Carlsson
Uppsala University
Chemistry Department
Box 531
S-75121 Uppsala Sweden

Prof. David S. Dandy
Dept. of Agricultural and Chemical Engineering
Colorado State University
Fort Collins, CO 80523

Prof. Robert F. Davis
Dept. of Materials Science and Engineering
North Carolina State University
229 Riddick Laboratories
Raleigh, NC 27695

Professor Seshu B. Desu
Department of Materials Science and Engineering
Virginia Polytechnic Institute
213 Holden Hall
Blacksburg, VA 24061-0140

Prof. James Edgar
Department Chemical Engineering
Kansas State University
Manhattan, Kansas 66506-5102

Prof. James W. Evans
Dept. of Materials Science and Mineral Engineering
University of California
Berkeley, CA 94720

Prof. Richard C. Flagan
Environmental Engineering
California Institute of Technology
138-78
Pasadena, CA 91125

Prof. Arthur Fontijn
Dept. of Chemical Engineering
Rensselaer Polytechnical Institute
110 8th Street
Troy, NY 12180-3590

Prof. Michael Frenklach
Dept. of Materials Science and Engineering
Pennsylvania State University
202 Academic Projects Building
University Park, PA 16802

Prof. Bernard Gallois
Dept. of Materials Science
Stevens Institute of Technology
Castle Point on the Hudson
Boboken, NJ 07030

Prof. Roy G. Gordon
Department of Chemistry
Harvard University
Mallinckrodt Laboratory
12 Oxford Street
Cambridge, MA 02138

Dr. Robert H. Hauge
Dept. of Chemistry
Rice University
Houston, TX 77251

Prof. Peter Hess
Institut fur Physikalische Chemie
Heidelberg University
Im Neuenheimer Feld 253
69120 Heidelberg
Germany

Prof. Robert F. Hicks
Department of Chemical Engineering
UCLA
5531 Boelter Hall
Los Angeles, CA 90095-1592

Prof. Klavs F. Jensen
MIT
Department of Chemical Engineering
RM66-566
77 Massachusetts Ave.
Cambridge, MA 02139-4307

Professor D. Lynn Johnson
Dept. Of Materials Science & Engineering
Northwestern University
The Technological Institute
Evanston, IL 60201

Prof. Linda Jones
NYS College of Ceramics
Alfred University
2 Pine Street
Alfred, NY 14802

Professor Joseph L. Katz
Chemical Engineering
Johns Hopkins University
Charles and 34th Streets
Baltimore, MD 21218

Prof. Keith King
Department of Chemical Engineering
University of Adelaide
Adelaide, SA
Australia 5005

Prof. H. Komiyama
Department of Chemical Engineering
University of Tokyo
Hongo 7, Bunkyo-ku
Tokyo 113
Japan

Dr. F. Langlais
Laboratoire des Composites
Thermostructuraux
Domaine Universitaire
33600 Pessac
France

Prof. M.C. Lin
Department of Chemistry
Emory University
Atlanta, GA 30322

Prof. Paul Marshall
Department of Chemistry
University of North Texas
P.O. Box 5068
Denton, TX 76203-5068

Prof. R.E. Mitchell
Dept. of Mechancial Engineering
Stanford University
Stanford, CA 94305

Prof. Philip W. Morrison, Jr.
Dept. of Chemical Engineering
Case Western Reserve University
10900 Euclid Avenue
Cleveland, OH 44106-7217

Prof. Triantafillos J. Mountziaris
Chemical Engineering Dept.
SUNY Buffalo
Buffalo, NY 14260

Prof. Zuhair A. Munir
Department of Mechanical Engineering
University of California
Davis, CA 95616

Prof. Clifford E. Myers
State University of New York at
Binghamton
Department of Chemistry
Binghamton, NY 13901

Dr. Roger Naslain
Laboratoire des Composites
Thermostructuraux
Domaine Universitaire
33600 Pessac
France

Dr. Michel Pons
Laboratoire de Science des Surfaces et
Materizux Carbones
Institu National Polytechnique de
Grenoble
ENSEED
38402 Saint-Martin-d'Heres Cedex
France

Prof. S.E. Pratsinis
Chemical & Nuclear Engineering
University of Cincinnati
627 Rhodes Hall, Mail Loc. 171
Cincinnati, OH 45221-0171

Prof. Daniel E. Rosner
Chemical Engineering Dept.
Yale University
P.O. Box 2159, Yale Station
New Haven, CT 06520-2159

Prof. Adel Sarofim
Department of Chemical Engineering
Massachusetts Institute of Technology
66-466
Cambridge, MA 02139

Prof. Brian W. Sheldon
Division of Engineering
Brown University
Box D
Providence, RI 02912

Dr. Daniel J. Skamser
Dept. of Materials Science and Engineering
Northwestern University
MLSF 2036
Evanston, IL 60208-3108

Prof. Stratis V. Sotirchos
Dept. of Chemical Engineering
University of Rochester
Rochester, NY 14627-0166

Prof. Karl E. Spear
Dept. of Ceramic Science and Engineering
Pennsylvania State University
201 Steidle Building
University Park, PA 16802

Prof. Thomas L. Starr
Room 113
Baker Building
Georgia Institute of Technology
Atlanta, GA 30332-0245

Professor Stan Veprek
Institute of Chemistry of Information Recording
Technical University of Munich
Lichtenbergstrasse 4
D-8046 Barching-Munich
Germany

Dr. Thomas H. Baum
Advanced Technology Materials
7 Commerce Drive
Danbury, CT 06810-4169

Dr. H.F. Calcote
Director of Research
Aerochem Research Laboratories
P.O. Box 1
Princeton, NJ 08542

Dr. Ali S. Fareed
Lanxide Corporation
1300 Marrows Road
P.O. Box 6077
Newark, DE 19714-6077

Dr. Douglas W. Freitag
DuPont Lanxide Composites, Inc.
17 Rocky Glen Court
Brookeville, MD 20833

Dr. Jitendra S. Goela
Morton Advanced Materials
185 New Boston Street
Woburn, MA 01801-6278

Dr. Christopher J. Griffin
3M Corporation
3M Center, Building 60-1N-01
St. Paul, MN 55144-1000

Dr. Stephen J. Harris
Physical Chemistry Dept.
GM Research and Development
30500 Mound Road 1-6
Warren, MI 48090-9055

Dr. Mark H. Headinger
DuPont Lanxide Composites, Inc.
400 Bellevue Road, P.O. Box 6100
Newark, DE 19714-6100

Dr. James Loan
MKS Instruments, Inc.
6 Shattuck Road
Andover, MA 01810

Dr. K.L. Luthra
General Electric Corporate Research and Development
Room 3B4, Building K1
Schenectady, NY 12301

Dr. Richard J. McCurdy
Libbey-Owens-Ford Co.
1701 East Broadway
Toledo, OH 43605

Dr. Meyya Meyyappan
Scientific Research Associates
50 Nyde Road
Glastonbury, CT 06033

Dr. Thomas H. Osterheld
Applied Materials, Inc.
Mail Stop 1510
Santa Clara, CA 95054

Mr. Peter Reagan
Project Manager, CVD Composites
Thermo Trex Corporation
74 West Street, P.O. Box 9046
Waltham, MA 02254-9046

Dr. David Roberts
J.C. Schumacher
1969 Palomar Oaks Way
Carlsbad, CA 92009

Dr. Andrew J. Sherman
Ultramet
12173 Montague Street
Pacoima, CA 91331

Dr. Richard Silberglitt
Technology Assessment and Transfer, Inc.
133 Defense Highway, #212
Annapolis, MD 21401

Dr. Bruce H. Weiller
Mechanics and Materials Technology
Center Aerospace Corporation
P.O. Box 92957
Los Angeles, CA 90009-2957

MS0349 S.T. Picraux, 1112

MS0601 W.G. Breiland, 1126

MS0601 M.E. Coltrin, 1126

MS0601 P. Esherick, 1126

MS0601 P. Ho, 1126

MS1349 R.E. Loehman, 1808

MS1393 D.W. Schaefer, 1814

MS0457 R.J. Eagan, 5600

MS0702 D.E. Arvizu, 6200

MS0710 G.A. Carlson, 6211

MS9003 T.O. Hunter, 8000
Attn: 8200 R.J. Detry
8400 L.A. Hiles

MS9214 C.F. Melius, 8117

MS9056 W.J. McLean, 8300
Attn: 8302 W. Bauer
8355 G. Fisk
8362 R. Carling
8366 B. Gallagher

MS9161 R.H. Stulen, 8342

MS9042 C.M. Hartwig, 8345
Attn: E. Evans
S. Griffiths
W.G. Houf
R. Nilson

MS9161 D.A. Outka, 8347

MS9162 A.E. Pontau, 8347

MS9055 F.P. Tully, 8353

MS9052 M.D. Allendorf, 8361 (10)

MS9052 D.R. Hardesty, 8361 (5)

MS9401 M.T. Dyer, 8700
Attn: 8711 M.W. Perra
8712 M.I. Baskes
8713 J.C.F. Wang
8715 G.J. Thomas
8716 K.L. Wilson
8717 W.G. Wolfer

MS9042 R.J. Kee, 8745

MS9042 R. Larson, 8745

MS9042 E. Meeks, 8745

MS9021 Technical Communications Department, 8535, for OSTI (10)

MS9021 Technical Communications Department, 8535/Technical Library, MS0899, 13414

MS0899 Technical Library, 13414 (4)

MS9018 Central Technical Files, 8523-2 (3)

Org.	Bldg.	Name	Rec'd by	Org.	Bldg.	Name	Rec'd by

LS 2900-QE

Sandia National Laboratories